Journal of Applied Physics

Photo-assisted Kelvin probe force microscopy investigation of three dimensional GaN structures with various crystal facets, doping types, and wavelengths of illumination

Cite as: J. Appl. Phys. **122**, 085307 (2017); https://doi.org/10.1063/1.5000137
Submitted: 03 May 2017 . Accepted: 13 August 2017 . Published Online: 25 August 2017

Manal Ali Deeb, Johannes Ledig, Jiandong Wei, Xue Wang, Hergo-Heinrich Wehmann, and Andreas Waag

Photo-assisted Kelvin probe force microscopy investigation of three dimensional GaN structures with various crystal facets, doping types, and wavelengths of illumination

Manal Ali Deeb,[1,a)] Johannes Ledig,[1,2,3] Jiandong Wei,[4] Xue Wang,[5] Hergo-Heinrich Wehmann,[1,2] and Andreas Waag[1,2]
[1]*Institut für Halbleitertechnik and Laboratory for Emerging Nanometrology, Technische Universität Braunschweig, 38092 Braunschweig, Germany*
[2]*Epitaxy competence center ec², Hans-Sommer-Straße 66, 38106 Braunschweig, Germany*
[3]*Physikalisch-Technische Bundesanstalt (PTB), Bundesallee 100, 38116 Braunschweig, Germany*
[4]*Institute of Nanochemistry and Nanobiology, Shanghai University, Shanghai 200444, People's Republic of China*
[5]*Osram Opto Semiconductors GmbH, Leibnizstraße 4, 93055 Regensburg, Germany*

(Received 3 May 2017; accepted 13 August 2017; published online 25 August 2017)

Three dimensional GaN structures with different crystal facets and doping types have been investigated employing the surface photo-voltage (SPV) method to monitor illumination-induced surface charge behavior using Kelvin probe force microscopy. Various photon energies near and below the GaN bandgap were used to modify the generation of electron–hole pairs and their motion under the influence of the electric field near the GaN surface. Fast and slow processes for Ga-polar c-planes on both Si-doped n-type as well as Mg-doped p-type GaN truncated pyramid micro-structures were found and their origin is discussed. The immediate positive (for n-type) and negative (for p-type) SPV response dominates at band-to-band and near-bandgap excitation, while only the slow process is present at sub-bandgap excitation. The SPV behavior for the semi-polar facets of the p-type GaN truncated pyramids has a similar characteristic to that on its c-plane, which indicates that it has a comparable band bending and no strong influence of the polarity-induced charges is detectable. The SPV behavior of the non-polar m-facets of the Si-doped n-type part of a transferred GaN column is similar to that of a clean c-plane GaN surface during illumination. However, the SPV is smaller in magnitude, which is attributed to intrinsic surface states of m-plane surfaces and their influence on the band bending. The SPV behavior of the non-polar m-facet of the slightly Mg-doped part of this GaN column is found to behave differently. Compared to c- and r-facets of p-type surfaces of GaN-light–emitting diode micro-structures, the m-plane is more chemically stable. *Published by AIP Publishing.* [http://dx.doi.org/10.1063/1.5000137]

I. INTRODUCTION

Three dimensional (3D) GaN micro- or nanostructures are very interesting candidates for both sensors and core-shell light–emitting diodes (LEDs).[1–7] This is due to the low defect density because of the reduced influence of the substrate concerning lattice and thermal mismatch. In comparison to conventional planar film LEDs, 3D micro- and nanorod LEDs can profoundly increase the active area on a given wafer area, by wrapping n-type GaN nanorods with InGaN quantum wells (QWs) and an outer shell of the p-type GaN. A further advantage of the 3D structures is that the major InGaN/GaN multi quantum well (MQW) area is located on non-polar m-plane sidewalls. The potential benefits of employing non-polar or semi-polar orientations for LED fabrication have been extensively demonstrated in recent years. Traditional MQWs grown on the polar c-plane suffer from the quantum confined Stark effect (QCSE).[8] The spontaneous and the piezoelectric polarization fields lead to a tilt of the band edges inside the quantum film and, thus, to a reduced overlap of the electron and hole wave functions. This leads to a less probable radiative recombination when the polarization fields are not fully screened by injected charge carriers. On non-polar surfaces, these fields are parallel to the QW and, thus, there is no QCSE. Therefore, a radiative recombination of electrons and holes in the QW is more probable. On semi-polar surfaces, the electrical polarization can be reduced or can even vanish too. On the other hand, the difference between these surfaces with respect to their electrical polarity is expected to affect their surface electronic properties[9] such as band bending[10] and subsequently on the mechanisms of charge transport induced by the absorption of photons or gas adsorption. The surface is especially crucial for GaN based nanowire gas sensors, where the intentional variation of surface band bending directly leads to a modulation of the sensing behavior.[11]

Wurtzite GaN films grown along the [0001] direction, i.e., c-plane films, have polar surfaces with spontaneous polarization of $-0.029\,\mathrm{cm}^{-2}$.[12] This induces a large negative surface charge for Ga-polar films and a positive charge for N-polar films.[13] These charges at polar crystal surface are one reason for the surface band bending, which is expected to be lower for N-polar GaN than for Ga-polar surface.[14] Another reason for band bending are charged surface states. Commonly, upward

a)Electronic mail: m.ali-deeb@tu-braunschweig.de

band bending due to negative charges at the surface and downward band bending due to positive charges at the surface are observed in n- and p-type semiconductors, respectively.[15] Surface states of GaN are formed due to Ga or N termination, surface reconstructions, native defects,[16] adsorbates, and oxidation.[17,18] It is widely accepted that a thin (~1 nm) Ga_2O_3 layer[17] as well as a monolayer of chemisorbed oxygen covers the GaN surface in air.[18] Traditionally,[15,19] surface states in semiconductors are classified into two types. The first type is considered to exist at the interface between the semiconductor and its native oxide. A charge transport process via these states is commonly expected to be fast.[20] The second type of states on the other hand is located on or within the surface oxide layer and is affected by the ambient atmosphere.[21,22] Charge exchange with the bulk occurs slowly, with a large time constant, typically of the order of seconds or more, and hence, these states are usually called slow state.[22] Both types are suggested to contribute to surface band bending in GaN near its surface,[21–24] and they also contribute to the surface photovoltage (SPV), i.e., the change of band bending on illumination.[19,25,26] In the case of n-GaN, this is due to the electric field driven accumulation of photo-generated holes at the surface where they screen the negative surface charges and, thus, reduce the band bending. This illumination-induced change of the surface voltage, i.e., the SPV, can be measured by photo-assisted Kelvin probe force microscopy (KPFM).[14,15,27] By applying lower incident photon energies, SPV measurements can also be used to determine the energy position of surface states.[28] In addition, this technique is also considered a powerful method that allows to distinguish between fast and slow charge transport processes into surface states. Various studies reported about these processes on GaN layers.[29,30] For example, Foussekis *et al.* investigated the fast and slow SPV responses in different gas environments using a single wavelength for both doped and undoped GaN layers. The SPV changes and, thus, the band bending under continuous illumination are explained by photo-induced adsorption of surface species in air ambient and photo-induced desorption in vacuum.[29] Reshchikov *et al.* reported about fast and slow processes and their contribution in SPV decay after illumination with high and low illumination intensities for an undoped GaN layer. It is shown that fast processes, i.e., accumulation of photo-generated holes at the semiconductor surface states and their recombination with electrons passing over the barrier, dominate at low illumination intensity (for both above- and below-bandgap excitation). On the other hand, the SPV decay in dark after ceasing above-bandgap illumination with sufficient intensity is qualitatively explained by the contribution of slow processes such as photo-induced adsorption and charging of a surface oxide layer.[20] In contrast to these measurements performed on GaN layers, two studies have been reported about SPV processes for Ga-polar and N-polar GaN nanorod/self-assembled nanowire using one wavelength.[24,31] Both of them demonstrated that the fast process for Ga-polar surfaces is larger than that for N-polar ones. This is attributed to the different initial band bending influenced by spontaneous polarization for the different polarities. The difference between these two studies was a large change of the slow process for the N-polar nanorod, whereas the slow process was absent on the N-polar nanowire. This behavior is ascribed to the presence of an oxide layer at the surface that hinders the electron transfer from the surface to the physisorbed oxygen, preventing chemisorption.

However, all mentioned results were measured on polar GaN surfaces using a single wavelength, and to date, no comprehensive work on other crystal orientations which normally appear with 3D GaN structures has been published. Additionally, especially in sensor applications but also in other 3D devices, differently doped surface areas appear with more or less influence on the device's performance. Thus, their electronic properties also concerning possible response times are of interest. The present work fills this gap and summarizes the behavior of fast and slow charge transport processes measured on 3D GaN structures with different types of doping and crystal orientation, using various – even sub-band-gap – wavelengths of illumination during photo-assisted Kelvin probe force microscopy.

II. EXPERIMENT

Different types of 3D GaN samples were studied in this work: 1) n-type GaN micro-structures, 2) GaN-based LED micro-structures, and 3) high aspect ratio GaN columns with a doping profile along the column's axis. All of the three samples investigated here were fabricated in a Thomas Swan metal organic vapor phase epitaxy (MOVPE) system. The GaN micro-structures of sample 1 were grown on a Si(110) substrate patterned with a SiO_x mask (30 nm thick) by means of a AlN nucleation layer (200–300 nm) and GaN nucleation. During the growth of the GaN core structures, silane (SiH_4) was injected for n-type doping. For the LED micro-structure of sample 2, the same process steps were applied as for sample 1, while in the 3D-growth also shell layers forming a 3-fold InGaN/GaN quantum well (QW) and a p-type Mg-doped GaN wrapped around the core were added. The vertically aligned GaN columns of sample 3 were grown on a GaN buffer (5.5 μm)/sapphire template patterned by a SiO_x mask (30 nm thick). This high aspect ratio columns were grown with an initial silane flow of 330 nmol/min for the first 360 s followed by a growth section with low Mg doping (50 nmol/min) for 700 s and a final 240 s growth section with again SiH_4 (330 nmol/min). In order to get access on the non-polar sidewalls, the columns were detached from their substrate. For this an n-type Si (111), wafer with a spin-coated conductive polymer film (Clevios™ PEDOT) was baked on a hotplate for 5 min at 130 °C. The columns of sample 3 were removed from their growth template by means of a scalpel, dropped onto this polymer surface, and baked again for 1 min to ensure a good physical and electrical connection. We assume that this procedure did not alter the surface properties at least of the upper three m-planes.

The samples' morphology was evaluated by a Stereoscan S360 scanning electron microscope using an acceleration voltage of 20 kV for the first and second sample and by a Zeiss supra 35 field emission scanning electron microscope (FESEM) using an acceleration voltage of 2 kV for the third sample. A Dimension 3100 scanning probe microscope (Veeco Instruments Inc.) was employed for KPFM measurements in air ambient. Commercial silicon tips with Pt/Ir coating

(PPP-EFM-Tip, Nanosensors) were used as a probe. The KPFM measurements were performed after a cleaning procedure of the samples with buffered hydrofluoric acid for 5 min in order to remove surface oxides and other contaminations.[32] The SPV was measured by illuminating the sample from the front side under grazing incidence. Commercial LEDs with peak wavelengths of 365 nm, 395 nm, and 470 nm were employed for this purpose. The 365 nm LED was chosen for band-to-band excitation of electrons since its absorption in the surface depletion region is substantial due to the Franz-Keldysh effect,[20,21] whereas the other wavelengths cause near-bandgap and sub-bandgap excitation. In order to get comparable SPV data for the different wavelengths, a similar photon flux density of the illumination ($\sim 10^{15}\,\mathrm{cm}^{-2}\,\mathrm{s}^{-1}$) was set by using different driving currents of the LEDs, which were defined beforehand by power density measurements using a fiber coupled spectrometer (Ocean Optics Inc. HR4000) and spectral sensitivity correction. The sample under test was kept in dark to minimize the residual potential from a previous light exposure. SPV data were acquired on the c-plane Ga-polar of both structures, n-type GaN and GaN-based LED. Additionally, SPV signals were measured on the inclined side facets of GaN-based LED truncated pyramidal structures using the illumination for band-to-band excitation. This illumination was also used for measuring SPV on the lying high aspect ratio columns in order to get information about the different doping zones along their length.

III. RESULTS AND DISSCUSION

Figure 1(a) schematically shows the energy diagram of the KPFM experiment to clarify the results. The contact potential difference eV_{CPD} between the metal tip of the scanning probe (left side) and the GaN surface (right side) corresponds to the difference in their work functions $(\emptyset_{tip} - \emptyset_{GaN})$. The work function of the semiconductor $\emptyset_{GaN} = \chi_{GaN} + \Phi_0 + E_{C-F}$ includes the electron affinity χ_{GaN}, the surface band bending Φ_0, and the difference E_{C-F} between the conduction band edge E_C and the Fermi level E_F in the bulk. eV_{CPD} is related to the band bending (Φ_0) of the GaN surface according to Eq. (1)

$$eV_{CPD} = \emptyset_{tip} - \emptyset_{GaN} = \emptyset_{tip} - \chi_{GaN} - \Phi_0 - E_{C-F}, \quad (1)$$

where e is the electron's charge. Assuming $\emptyset_{tip}$, χ_{GaN}, and E_{C-F} are constant, a variation in V_{CPD} is mainly related to the variation of the surface band bending, which is determined by sign and quantity of accumulated surface charges. The measured *SPV* of a sample corresponds to the change in band bending during illumination [cf. dashed curves in Fig. 1(a)]

$$eSPV = \Phi_0 - \Phi_{light}, \quad (2)$$

where Φ_0 indicates the value obtained in dark (solid black curves), whereas Φ_{light} denotes the value obtained during illumination (dashed red curves). For this non-equilibrium state, the quasi Fermi levels are shown schematically as dotted curves in red. They represent the increase in electron and hole concentrations due to ongoing photo generation and the related drift, diffusion, and recombination. Figure 1(b) shows schematic drawings of band diagrams near the n-type GaN surface illustrating the fast and slow processes during illumination for band-to-band excitation (top), and of the energy

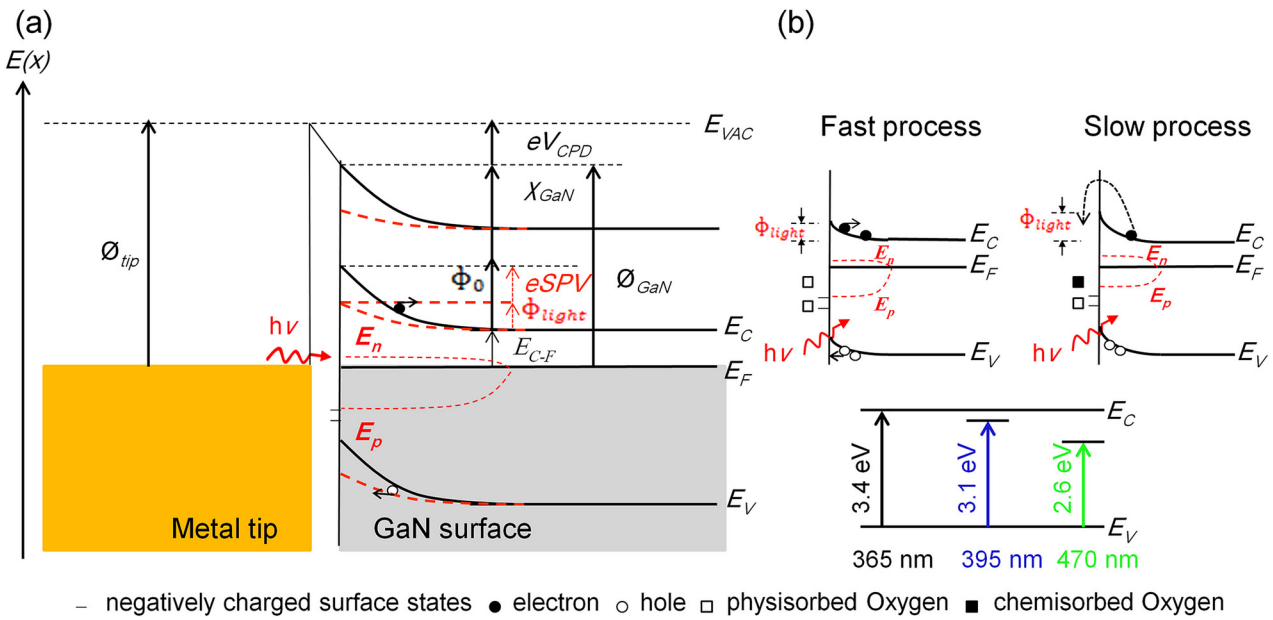

FIG. 1. (a) Schematic band diagram during KPFM with metal tip on the left and clean GaN on the right in air ambient. Band bending in dark and under illumination are depicted in solid (black) and dashed lines (red), respectively, (b) schematic drawings of band bending near the GaN surface illustrate the contribution of fast and slow processes during SPV measurements with illumination for band-to-band excitation (top) and schematic drawings of the energy gap that photons with a wavelength of 365, 395, and 470 nm, respectively, can reach (bottom). Fast process: photogenerated electron-hole pairs are separated by the electric field in the depletion zone (left figure). Holes are swept to the surface by the depletion field and screen negatively charged surface states. This accumulation of holes on the surface compensates the negatively charged surface states and reduces the upward bending (top left figure of b). This non-equilibrium situation is depicted schematically by separate quasi Fermi levels for electrons $\boldsymbol{E_n}$ and holes $\boldsymbol{E_p}$, as illustrated. Slow process: physisorbed oxygen species become chemisorbed by receiving electrons from the bulk over the decreased near-surface barrier which leads to negative charges on the surface increasing the band upwards bending (photo-induced chemisorption) (top right figure of b).

gap that photons with a wavelength of 365, 395, and 470 nm, respectively, can reach (bottom). The top left diagram comprises the electron-hole-pair generation when the illumination begins. The pairs are separated by the electric field in the depletion zone. Electrons move towards the bulk and holes towards the surface. When the holes accumulate at the surface, they partly screen the negatively charged surface states, and decrease the initial amount of the upwards band bending which is a fast process. The diagram on the top right side of Fig. 1(b) depicts photons exciting electrons from the conduction band over the remaining Schottky barrier to the physisorbed oxygen species on the surface which then become chemisorbed species. This slow process (photo-induced chemisorption) accumulates negative charges on the surface, increasing the upwards band bending.[20] However, illumination with near- or below-bandgap photons can excite electrons at surface states to overcome the surface barrier where they are swept into the bulk by the electric field of the depletion zone (not drawn here). This leads to a fast reduction of the band bending too. P-type GaN surfaces show an opposite behavior (not drawn here). In this case, the downwards band bending is reduced under band-to-band excitation because the electrons of the generated electron-hole pairs drift to the surface due to the electric field in the depletion region. On the other hand, illumination with near- or below-bandgap photons can excite holes from surface states into the bulk, compensating the existing charge of surface states and reducing the initial amount of downwards band bending. Both are fast processes.

Figures 2(a) and 2(c) show scanning electron micrographs of the examined 3D GaN samples with different doping, n- and p-type, respectively, tilted by 30° and the SiO_x growth mask still present between the truncated pyramidal GaN structures.

Figures 2(b) and 2(d) are atomic force microscopy (AFM) topographic images of a single n-type Si-doped and p-type Mg-doped GaN truncated pyramids, respectively, showing a top c-plane where SPV data were acquired. The white arrows correspond to the deviation of the averaged normal to the respective surface area relative to the c-axis, simplifying the identification of different surface orientations.

The SPV behavior of n-type GaN core micro-structures and p-type GaN shell of LED micro-structures under various wavelengths of illumination is shown in Fig. 3. After switching on the illumination with the two shorter wavelengths, i.e., 365 nm (black curve) and 395 nm (blue), the behavior of both samples is similar: for n-type GaN [Fig. 3(a)] an immediate increase in the absolute SPV value by about 195 mV and 75 mV, and for p-type GaN [Fig. 3(b)] an immediate decrease in the SPV by about 165 mV and 60 mV is observed, respectively. This immediate SPV response in both cases is followed by a slower decrease during further illumination. This latter is also visible for the longest wavelength of 470 nm [green curve in Fig. 3(a)]. However, in this case no immediate response after switching on the light is identified. Thus, we conclude that there is no significant compensation of surface states neither by photogenerated holes nor by direct excitation in this case of sub-bandgap illumination[28] mainly due to a low absorption efficiency for this wavelength. Similar

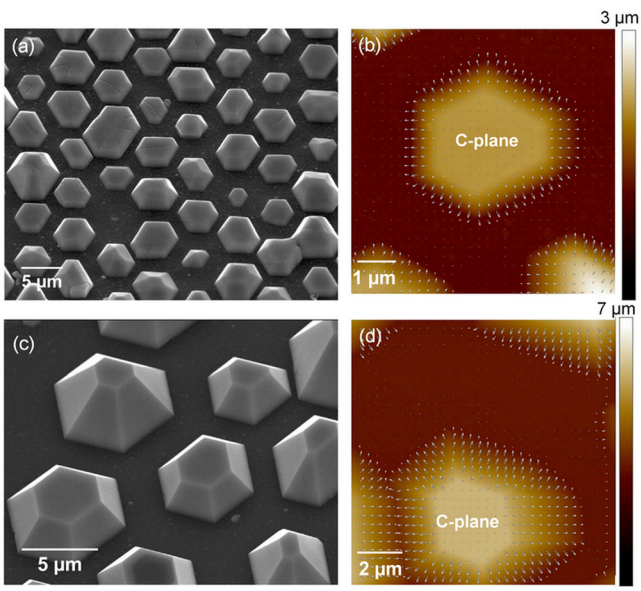

FIG. 2. Scanning electron microscope (SEM) images (30° tilted) on the left and atomic force topography images with gradient field overlaid in white on the right of [(a) and (b)] n-type GaN core micro-structures; [(c) and (d)] GaN-based LED micro-structures with p-type surfaces.

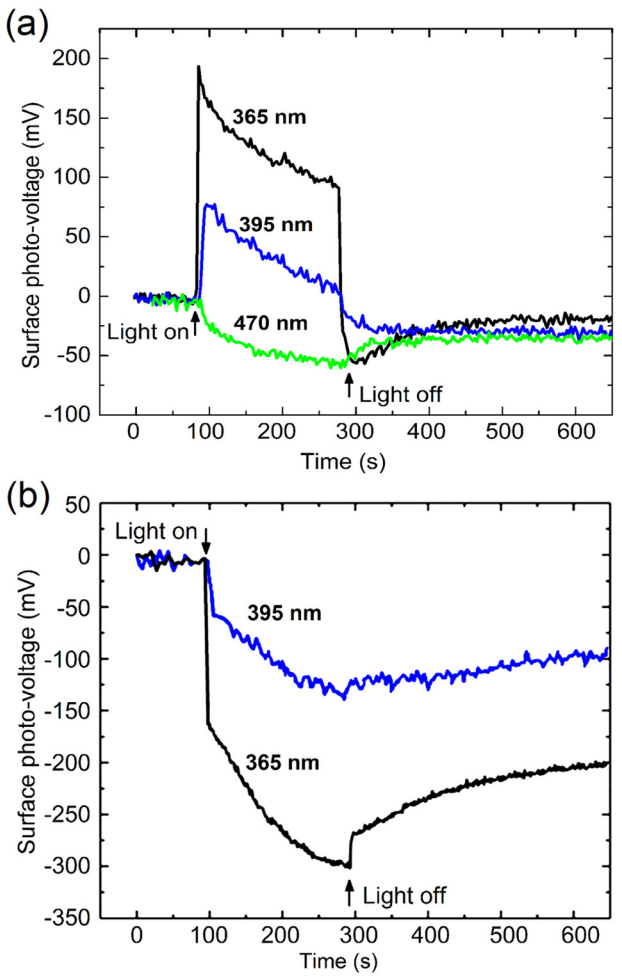

FIG. 3. SPV evolution of the top c-facet of (a) n-type GaN core micro-structure, (b) of p-type GaN-based LED micro-structure upon illumination for band-to-band (black), near-bandgap (blue), and sub-bandgap (green, only in a) excitation.

SPV behavior upon illumination with 470 nm is also expected for p-type GaN.

With regard to p-type GaN micro-structures the immediate decrease in the SPV is related to a partial compensation of positively charged surface states by photogenerated electrons for band-to-band illumination, or also by direct excitation of holes from surface states into the bulk for near-bandgap illumination, which both results in a fast decrease of the downwards band bending. This behavior for SPV on micro-structures is similar to that previously reported on the c-plane of n- and p-type GaN layers using an illumination with 325 nm[33] which indicate that the same surface states, located at about 1.3–1.5 eV below the conduction band, could be responsible for the upward and downward band bending for both, n- and p-type GaN, respectively, and, thus, for the opposite polarity of the fast SPV behavior. However, the SPV fast jumps for p-type were smaller than those for n-type, which can be ascribed to the pn-junction of the underlying LED structure with a second depletion zone and opposite electric field. Although the photon fluxes in our experiments were similar to another, the initial SPV rise upon band-to-band excitation is significantly larger than that upon near-bandgap excitation.

This observation is in agreement with the results of Reshchikov *et al.* obtained on GaN layers[20] and is a result of a smaller interaction efficiency of the sub-bandgap photons with the semiconductor. Obviously, the 470 nm photons do not have enough energy for introducing a significant screening of the charged surface states.

It is also worth noting that the amplitude difference of the immediate response between the two shorter wavelengths for p- and n-type GaN pyramidal structures is similar (about 120 and 105 mV, respectively) and also fits to the results of Foussekis *et al.*[34] This comparability between the results indicates that the surface states play a dominating role other than the doping.

After the fast initial response, the SPV signal of both 3D GaN surfaces shows a negative decay under continuous illumination for all three wavelengths (cf. Fig. 3). This slow decrease is attributed to the photo-induced chemisorption of oxygen as depicted in Fig. 1(b, right diagram).[20,29,30,35] In this process, physisorbed oxygen species become chemisorbed by receiving electrons from the bulk. In the case of band-to-band excitation, the electrons can overcome the reduced near-surface barrier. In the case of sub-bandgap excitation, they are directly excited over the initially unchanged barrier. In both cases, the accumulation of negatively charged surface species results in an upward band bending for n- and p-type GaN and the observed decrease in SPV.[33] The energy needed for the transformation of physisorbed to chemisorbed oxygen is obviously lower than the 2.6 eV provided by the 470 nm photons.

Additionally to these measurements on the top c-facet of the GaN LED structure, the SPV behavior of the semi-polar side-facets of the truncated, hexagonal pyramids was measured and compared to the SPV taken at the top c-facet. Figure 4(a) shows a perspective AFM image of a single truncated pyramid LED micro-structure. The side-facets appear at an angle of approximately 60° to the (0001) top plane and, thus, correspond to the semi-polar $\{1\bar{1}01\}$ facets.[36] The

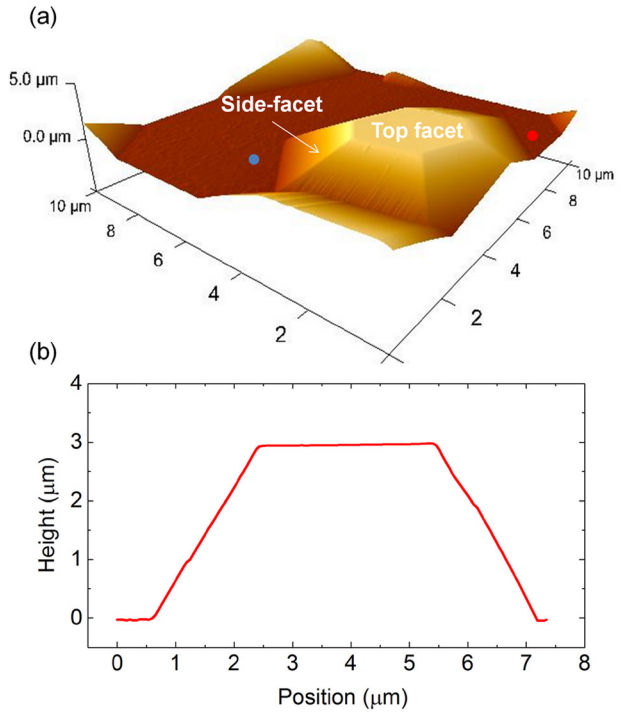

FIG. 4. (a) Perspective view ($10 \times 10\ \mu m^2$) of the AFM topography of a typical truncated pyramid structure showing the facets of GaN-based LED micro-structure on which the SPV was measured; (b) its cross-section, which was taken from blue to red dot.

profile across the truncated pyramid taken from the blue to the red dot in Fig. 4(a) shows the inclination of semipolar facets as depicted in Fig. 4(b).

Compared to the SPV signal of the semi-polar facet (red curve), the corresponding signal of the polar top facet (black curve) in Fig. 5 shows the same characteristics but a larger voltage swing with respect to band-to-band excitation. Although the SPV determined by KPFM theoretically does not depend on the geometry which is reflected by the gradient of the curve of the capacitance between tip and surface over their distance, the amplitude of the oscillating tip is controlled to zero. In practice, however, there is always a small signal left so that the measured SPV varies with changing

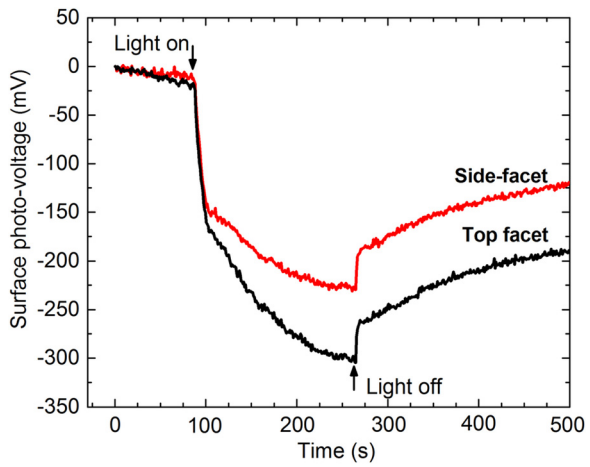

FIG. 5. SPV signal for top facet (black) and side-facet (red) of p-GaN on the LED micro-structure upon band-to-band excitation.

gradient. Especially, the tilted facet leads to a larger capacitance between KPFM tip and the semiconductor and, thus, to a different gradient. Additionally, the forces partly act in lateral direction on the cantilever which is not correctly detected by the used AFM system.[37] Therefore, the small difference between the SPV behaviors on the two examined facets could be ascribed more to the geometry of the microstructure than to an assumed reduced surface charge of semipolar facets due to its reduced polarity. This means that the SPV and subsequently the band bending of the semi-polar facet are comparable to the band bending of the polar top facet and confirm the important role of surface states in this behavior rather than polarization charges alone.[10] On the other hand, the observed small decay in both signals before turning on the light does not affect the main results mentioned here and can be ascribed to the remaining influence of a previous light exposure.

Additionally to the polar and semi-polar facets, the charge transfer processes have been investigated on the non-polar m-facets of 3D GaN columns from sample 3. Figure 6 presents the respective results taken on a high aspect ratio GaN column. The inset of Fig. 6(b) shows an SEM image of the as grown sample (tilted by 30°) with the SiO_x growth mask still present between the columns. The detached GaN column under study is illustrated in the AFM topography of Fig. 6(a), where the black, red, and blue dots on the differently doped parts (n-type bottom and upper part and p-type middle part) of the GaN column indicate the positions at which the SPV transients in Fig. 6(b) were measured. The white arrows in AFM image correspond to the deviation of the normal to the respective surface area relative to the c-axis, simplifying the identification of different surface orientations. Since the averaged gradient of the area under the arrows is shown, they stick out beyond the column.

This smaller voltage swing can only be assigned to a small extent to geometrical effects since in both cases the tip's vibration plane is perpendicular to the measured surface and only their lateral dimensions differ. Thus, in this case the reduced amplitude for SPV fast jump can be ascribed to a large extent to the surface electronic properties of the non-polar m-plane GaN. Obviously, a lower density of charged intrinsic surface states reduces the band bending[38–41] and subsequently the SPV amplitudes. The SPV behavior of the slightly Mg-doped middle section of the column [red curve in Fig. 6(b)] behaves different. The fast initial SPV increase is similar to the behavior of ends of the column (blue and black curve). Since for p-type GaN the fast SPV response should be negative, the slight Mg-doping was not sufficient to overcompensate the normally n-type background doping. Nevertheless, this middle part shows instead of a slow decrease of the SPV signal a constant value under illumination. This constant value suggests a chemically more stable surface or a smaller sensitivity to environmental conditions (air in this case). A similar SPV behavior during illumination was also measured on the undoped part of a GaN column where only the first part was grown with SiH_4-doping and the upper part without doping (not shown here). In both cases, the differences can clearly be ascribed to the semiconductor and not to the geometry.

According to a theoretical work,[42] the surfaces of the polar and semi-polar planes are hydrogen terminated for the MOVPE growth parameters used here, whereas the non-polar m-plane should be ideal without adsorption. Concerning doping, Mg is unlikely to be incorporated neither on the polar c-plane nor on the semi-polar planes for the 3D growth conditions used in our case. Since the GaN columns show no c-plane on top after and during growth, which means that c-plan grows so fast that it vanishes, and the columns end with semi-polar planes and look like a pencil; the m-planes do not grow at all so that the limiting planes are the semipolar ones during the 3D growth process.[43] Although Si was not analyzed on similar rods overgrown by an LED structure, a Si-rich layer was detected by transmission electron microscopy based energy dispersive X-ray spectroscopy as well as by Auger spectroscopy of the sidewall surface.[43] This Si-rich layer is believed to strongly influence the diffusion of growth species on the m-planes and, thus, promotes 3D growth. Since according to Ref. 42, the ideal m-plane surface of the not intentionally doped or slightly Mg-doped part of the columns clearly shows a chemically more stable surface. Obviously, the Si containing parts with their Si-rich surface are less stable.

IV. CONCLUSION

In conclusion, for the first time SPV signals were taken on the most prominent crystal facets and doping types which

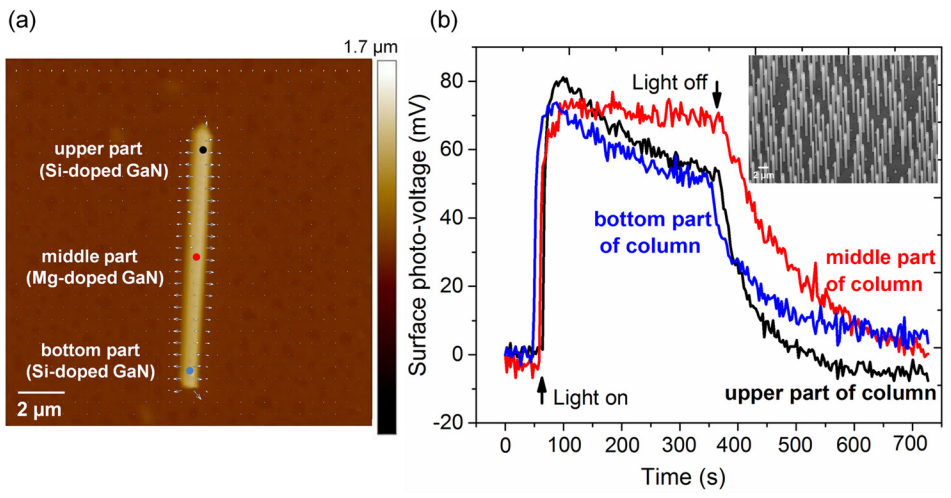

FIG. 6. (a) AFM topography map with gradient field overlaid in white of a single GaN column lying on a conductive polymer film: the upper and the bottom part are doped with Si, whereas the middle part is slightly Mg-doped; the black, red, and blue dots on the column illustrate the positions where the SPV was measured. (b) SPV evolution on the different parts of GaN column using band-to-band excitation (365 nm); inset: field emission scanning electron microscopy (FESEM) image of a well-aligned ensemble of GaN columns (30° tilted).

generally appear during the selective area MOVPE grown three dimensional Ga-polar GaN devices. Fast and slow SPV responses of the top c-facet of p- and n-type 3D GaN structures were clearly distinguished and compared under various excitation conditions. Illumination generates an immediate positive SPV response for n-type and a negative one for p-type 3D GaN micro-structures, which is consistent with the expected reduction of surface band bending for both surface types and with the studies on GaN layers. Fast processes are attributed to the accumulation of photo-generated minority carriers, i.e., holes for n-type and electrons for p-type, at the surface for band-to-band excitation, or are ascribed to the excitation of electrons (n-type) or holes (p-type) from surface states into the bulk for near-bandgap illumination. In the case of sub-bandgap illumination, only the photo-induced chemisorption of oxygen as a slow process is activated. Semi-polar facets of p-type GaN truncated pyramidal LED structures show a similar SPV behavior for that on their c-facet. However, its amplitude might be affected by the topography of the setup. This indicates that they have a comparable surface band bending and no strong influence of the reduced polarity induced charges could be detected. The SPV behavior for non-polar m-facets of Si doped n-type GaN columns is also similar to that on clean c-plane GaN surfaces during illumination. However, the SPV is smaller in magnitude, which is attributed to the different amount of surface states on m-planes. On the other hand, there is no slow SPV process on the not intentionally or slightly Mg-doped non-polar m-plane surface, indicating a higher chemical stability.

ACKNOWLEDGMENTS

This work has been funded by the EU project GECCO (Grant No. 280694). We are grateful to Dr. F. Hitzel (DME Nanotechnologie GmbH in Braunschweig) and Professor M. Tornow for giving us the ability to use the KPFM set-ups and Professor M. Schilling and Dr. F. Ludwig (TU Braunschweig) to use the FESEM set-up. We would like to thank A. Schmidt, D. Rümmler, K.-H. Lachmund, and M. Karsten from TU Braunschweig for their technical support.

[1]W. Bergbauer, M. Strassburg, C. Kölper, N. Linder, C. Roder, J. Lähnemann, A. Trampert, S. Fündling, S. F. Li, H.-H. Wehmann, and A. Waag, Nanotechnology **21**, 305201 (2010).
[2]A. Waag, X. Wang, S. Fündling, J. Ledig, M. Erenburg, R. Neumann, M. Al Suleiman, S. Merzsch, J. Wei, S. Li, H.-H. Wehmann, W. Bergbauer, M. Straßburg, A. Trampert, and H. Riechert, Phys. Status Solidi **8**, 2296 (2011).
[3]Y. J. Hong, C.-H. Lee, A. Yoon, M. Kim, H.-K. Seong, H. J. Chung, C. Sone, Y. J. Park, and G.-C. Yi, Adv. Mater. **23**, 3284 (2011).
[4]S. Li and A. Waag, J. Appl. Phys. **111**, 71101 (2012).
[5]M. Mandl, X. Wang, T. Schimpke, C. Kölper, M. Binder, J. Ledig, A. Waag, X. Kong, A. Trampert, F. Bertram, J. Christen, F. Barbagini, E. Calleja, and M. Strassburg, Phys. Status Solidi -Rapid Res. Lett. **7**, 800 (2013).
[6]X. Wang, S. Li, M. S. Mohajerani, J. Ledig, H.-H. Wehmann, M. Mandl, M. Strassburg, U. Steegmu, U. Jahn, J. Lähnemann, H. Riechert, I. Griffit, D. Cherns, and A. Waag, Cryst. Growth Des. **13**, 3475 (2013).
[7]G. Liu, B. Wen, T. Xie, A. Castillo, J.-Y. Ha, N. Sullivan, R. Debnath, A. Davydov, M. Peckerar, and A. Motayed, Microelectron. Eng. **142**, 58 (2015).
[8]P. Waltereit, O. Brandt, A. Trampert, H. T. Grahn, J. Menniger, M. Ramsteiner, M. Reiche, and K. H. Ploog, Nature **406**, 865 (2000).
[9]P. Reddy, I. Bryan, Z. Bryan, W. Guo, L. Hussey, R. Collazo, and Z. Sitar, J. Appl. Phys. **116**, 123701 (2014).
[10]I. Bartoš, O. Romanyuk, J. Houdkova, P. P. Paskov, T. Paskova, and P. Jiříček, J. Appl. Phys. **119**, 105303 (2016).
[11]A. Patsha, P. Sahoo, S. Amirthapandian, A. K. Prasad, A. Das, A. K. Tyagi, M. A. Cotta, and S. Dhara, J. Phys. Chem. C **119**, 21251 (2015).
[12]E. T. Yu, X. Z. Dang, P. M. Asbeck, S. S. Lau, and G. J. Sullivan, J. Vac. Sci. Technol. B **17**, 1742 (1999).
[13]O. Ambacher, J. Smart, J. R. Shealy, N. G. Weimann, K. Chu, M. Murphy, W. J. Schaff, L. F. Eastman, R. Dimitrov, L. Wittmer, M. Stutzmann, W. Rieger, and J. Hilsenbeck, J. Appl. Phys. **85**, 3222 (1999).
[14]J. D. Wei, S. F. Li, A. Atamuratov, H.-H. Wehmann, and A. Waag, Appl. Phys. Lett. **97**, 172111 (2010).
[15]L. Kronik and Y. Shapira, Surf. Sci. Rep. **37**, 1 (1999).
[16]W. E. Spicer, P. W. Chye, P. R. Skeath, C. Y. Su, and I. Lindau, J. Vac. Sci. Technol. **16**, 1422 (1979).
[17]T. Sasaki and T. Matsuoka, J. Appl. Phys. **64**, 4531 (1988).
[18]V. M. Bermudez, J. Appl. Phys. **80**, 1190 (1996).
[19]A. Many, Y. Goldstein, and N. B. Grover, *Semiconductor Surfaces* (North-Holland, Amsterdam, 1971), p. 77.
[20]M. A. Reshchikov, M. Foussekis, and A. A. Baski, J. Appl. Phys. **107**, 113535 (2010).
[21]M. A. Reshchikov, S. Sabuktagin, D. K. Johnstone, and H. Morkoc¸, J. Appl. Phys. **96**, 2556 (2004).
[22]O. Johnson, Phys. Rev. **111**, 153 (1958).
[23]O. Renault, J. Morin, P. Tchoulfian, N. Chevalier, V. Feyer, J. Pernot, and C. M. Schneider, Ultramicroscopy **159**, 476 (2015).
[24]J. Wei, R. Neumann, X. Wang, S. Li, S. Fündling, S. Merzsch, M. A. M. Al-Suleiman, Ü. Sökmen, H.-H. Wehmann, and A. Waag, Phys. Status Solidi **8**, 2157 (2011).
[25]R. H. Kingston, J. Appl. Phys. **27**, 101 (1956).
[26]W. H. Brattain and J. Bardeen, Bell Syst. Technol. J. **32**, 1 (1953).
[27]M. Nonnenmacher, M. P. O'Boyle, and H. K. Wickramasinghe, Appl. Phys. Lett. **58**, 2921 (1991).
[28]C. L. Balestra, J. Łagowski, and H. C. Gatos, Surf. Sci. **64**, 457 (1977).
[29]M. Foussekis, A. A. Baski, and M. A. Reshchikov, Appl. Phys. Lett. **94**, 162116 (2009).
[30]M. Foussekis, J. D. Ferguson, J. D. McNamara, A. A. Baski, and M. A. Reshchikov, J. Vac. Sci. Technol. B **30**, 51210 (2012).
[31]A. Minj, A. Cros, N. Garro, J. Colchero, T. Auzelle, and B. Daudin, Nano Lett. **15**, 6770 (2015).
[32]L. L. Smith, S. W. King, R. J. Nemanich, and R. F. Davis, J. Electron. Mater. **25**, 805 (1996).
[33]M. Foussekis, A. A. Baski, and M. A. Reshchikov, J. Vac. Sci. Technol. B **29**, 41205 (2011).
[34]M. Foussekis, J. D. Ferguson, A. A. Baski, H. Morkoç, and M. A. Reshchikov, Phys. B Condens. Matter **404**, 4892 (2009).
[35]T. Wolkenstein, *Electronic Processes on Semiconductor Surface During Chemisorption* (Consultants Bureau, New York, 1991).
[36]A. Lundskog, U. Forsberg, P. O. Holtz, and E. Janzén, Cryst. Growth Des. **12**, 5491 (2012).
[37]O. Vatel and M. Tanimoto, J. Appl. Phys. **77**, 2358 (1995).
[38]L. Ivanova, S. Borisova, H. Eisele, M. Dähne, A. Laubsch, and P. Ebert, Appl. Phys. Lett. **93**, 192110 (2008).
[39]M. Bertelli, P. Löptien, M. Wenderoth, A. Rizzi, R. G. Ulbrich, M. C. Righi, A. Ferretti, L. Martin-Samos, C. M. Bertoni, and A. Catellani, Phys. Rev. B **80**, 115324 (2009).
[40]L. Lymperakis, P. H. Weidlich, H. Eisele, M. Schnedler, J. P. Nys, B. Grandidier, D. Stiévenard, R. E. Dunin-Borkowski, J. Neugebauer, and P. Ebert, Appl. Phys. Lett. **103**, 152101 (2013).
[41]M. Himmerlich, A. Eisenhardt, S. Shokhovets, S. Krischok, E. Speiser, M. D. Neumann, A. Navarro-Quezada, and N. Esser, Appl. Phys. Lett. **104**, 171602 (2014).
[42]Y. Kangawa, T. Akiyama, T. Ito, K. Shiraishi, and T. Nakayama, Materials **6**, 3309 (2013).
[43]J. Hartmann, X. Wang, H. Schuhmann, W. Dziony, L. Caccamo, J. Ledig, M. S. Mohajerani, T. Schimpke, M. Bähr, G. Lilienkamp, W. Daum, M. Seibt, M. Straßburg, H.-H. Wehmann, and A. Waag, Phys. Status Solidi Appl. Mater. Sci. **212**, 2830 (2015).